

# Charge and Flux Noise from Nonequilibrium Quasiparticle Energy Distributions in Superconducting Wires

José Alberto Nava Aquino and Rogério de Sousa  
*Department of Physics and Astronomy, University of Victoria,  
 Victoria, British Columbia V8W 2Y2, Canada and  
 Centre for Advanced Materials and Related Technology,  
 University of Victoria, Victoria, British Columbia V8W 2Y2, Canada*  
 (Dated: August 1, 2024)

The quasiparticle density observed in low-temperature superconducting circuits is several orders of magnitude higher than the value expected at thermal equilibrium. The tunneling of this excess of quasiparticles across Josephson junctions is recognized as one of the main loss and decoherence mechanisms in superconducting qubits. Here we propose an additional loss mechanism arising from nonequilibrium quasiparticle densities: Ohmic loss due to quasiparticles residing in superconducting wires away from the junctions. Our theory leverages the recent experimental demonstration that the excess quasiparticles are in *quasiequilibrium* [T. Connolly *et al.*, *Phys. Rev. Lett.* **132**, 217001 (2024)] and uses a generalized fluctuation-dissipation theorem to predict the amount of charge and flux noise generated by them. We show that the resulting charge noise can be larger than dielectric loss due to amorphous two-level systems at frequencies in the MHz range, and find a logarithmic-in-frequency “nearly white” contribution to flux noise that is comparable to the flux noise observed in experiments. This shows that wire-resident quasiparticles are a universal source of loss and decoherence even when the quasiparticles are far away from Josephson junctions.

## I. INTRODUCTION

Superconducting (SC) qubits represent a promising pathway toward scalable quantum computing, leveraging the coherence of macroscopic quantum states [1]. A pivotal factor in their operational efficacy is maintaining quantum coherence, a challenge compounded by various decoherence mechanisms [2–7]. Among these, quasiparticles (QPs), excitations resulting from broken Cooper pairs, emerge as a concern. The presence of QPs in superconductors is known to give rise to surface resistance and Ohmic loss [8]. Their impact on SC qubits is believed to be the greatest when they tunnel across a Josephson junction (JJ), leading to energy relaxation and dephasing, thereby limiting qubit performance [9–12].

Several experiments show that a large population of nonequilibrium QPs remain even at low temperatures ( $k_B T \ll \Delta$ ), in spite of the thermal QP population being exponentially small ( $\propto e^{-\Delta/k_B T}$ , where  $\Delta$  is the SC energy gap) [13, 14]. These nonequilibrium populations are believed to arise from external perturbations, such as stray infrared photons or ionizing radiation [15, 16], posing a great challenge to qubit coherence. An additional unknown is the energy distribution for the nonequilibrium QPs. A recent experiment provided evidence of *quasiequilibrium*, where QPs are in thermal equilibrium with the surrounding phonon bath despite having an out-of-equilibrium density. Therefore, even though the QPs arise from high-energy sources, rapid inelastic processes mediated by phonons restore them to a thermal-like energy distribution [17].

Current designs of SC circuits engineer junction asymmetries in order to prevent QP tunneling across the circuit’s JJs, greatly reducing the impact of the QP tunneling mechanism [17–19]. Here we show that the Ohmic

loss induced by QPs within the SC wires themselves gives rise to charge and flux noise even when the QPs are far from the junctions. Our explicit numerical calculations suggest that the associated charge noise can be larger than the one arising from two-level systems (TLSs).

The resulting charge noise generates flux fluctuations due to the self-inductance of the wires, giving rise to a flux noise background that is logarithmic in frequency. The magnitude of the predicted “nearly white flux noise background” is found to be comparable to values observed in flux-tunable qubits [20, 21].

## II. CHARGE SUSCEPTIBILITY AND CONDUCTIVITY FROM QUASIPARTICLES

In this section we propose analytical approximations for the charge susceptibility in a superconducting circuit and the conductivity of its quasiparticle excitations. The linear response in a general circuit due to a small perturbation in voltage  $V$  is  $\delta V = Z \langle \delta I \rangle = -i\omega Z \langle \delta Q \rangle$ , where  $Z$  is a complex impedance. The charge susceptibility in a wire is thus given by  $\tilde{\chi}_Q(\omega) = \frac{\langle \delta Q \rangle}{\delta V} = -\frac{1}{i\omega Z}$ . In the presence of quasiparticle excitations, the wire possesses a frequency-dependent impedance  $Z(\omega) = \frac{\ell}{A\sigma(\omega)}$ , where  $\sigma(\omega) = \sigma_1(\omega) + i\sigma_2(\omega)$  is the SC’s complex conductivity, and  $\ell$ ,  $A$  are the wire’s length and cross-sectional area, respectively. The charge susceptibility due to the presence of QPs in a wire is then  $\tilde{\chi}_Q(\omega) = \frac{iA\sigma(\omega)}{\ell\omega}$  and its imaginary part is

$$\text{Im} \{ \tilde{\chi}_Q(\omega) \} = \frac{A\sigma_1(\omega)}{\ell\omega}. \quad (1)$$

The frequency-dependent conductivities of a Bardeen-Cooper-Schrieffer (BCS) superconductor were calculated

by Mattis and Bardeen in [8] for the case where the quasiparticles are at thermal equilibrium, with average occupation given by Fermi-Dirac functions  $f(E) = 1/(e^{E/k_B T} + 1)$ . Here  $E \equiv E_k = \sqrt{\xi_k^2 + \Delta^2}$  is the BCS quasiparticle energy, with  $\xi_k = \epsilon_k - \epsilon_F$  the free electron energy measured from the Fermi level  $\epsilon_F$ .

The Mattis-Bardeen theory can be generalized to the case away from thermal equilibrium, provided that quasiparticle occupation remains a function of QP energy  $E$ . We shall make this key *QP energy distribution assumption* and refer to the quasiparticle occupations as  $n(E)$ , a function that can differ from the equilibrium Fermi-Dirac function  $f(E)$ . The Mattis-Bardeen conductivities then become

$$\frac{\sigma_1}{\sigma_N} = \frac{2}{\hbar\omega} \int_{\Delta}^{\infty} dE \frac{E(E + \hbar\omega) + \Delta^2}{\sqrt{E^2 - \Delta^2} \sqrt{(E + \hbar\omega)^2 - \Delta^2}} \times [n(E) - n(E + \hbar\omega)], \quad (2a)$$

$$\frac{\sigma_2}{\sigma_N} = \frac{1}{\hbar\omega} \int_{\Delta - \hbar\omega}^{\Delta} dE \frac{E(E + \hbar\omega) + \Delta^2}{\sqrt{\Delta^2 - E^2} \sqrt{(E + \hbar\omega)^2 - \Delta^2}} \times [1 - 2n(E + \hbar\omega)]. \quad (2b)$$

These expressions are valid at subgap frequencies  $\hbar\omega < 2\Delta$ , with  $\sigma_N$  the non-SC (normal state) real part of the conductivity.

In order to connect to experiments, it is fruitful to express  $\sigma_1(\omega)$  in terms of the number of QPs divided by the number of electrons bound as Cooper pairs [10, 11, 22],

$$x_{\text{QP}} = \frac{N_{\text{QP}}}{2\rho\Delta} = \frac{1}{\Delta} \int_{-\infty}^{\infty} d\xi n(\sqrt{\xi^2 + \Delta^2}), \quad (3)$$

where  $\rho$  is the electron energy density near  $\epsilon_F$ . As we shall argue below, the QP occupation appears to follow a ‘‘quasithermal’’ law  $n(E) \approx n_0 e^{-E/k_B T}$  in experiments. Here  $n_0$  does not depend on QP energy  $E$  or frequency  $\omega$ , but it may depend on other parameters such as temperature  $T$  and gap  $\Delta$ . For the special case of thermal equilibrium we get  $n_0 = 1$ , as can be seen from  $n(E) = f(E) = 1/(e^{E/k_B T} + 1) \approx e^{-E/k_B T}$ . When the quasithermal law is followed and  $k_B T \ll \Delta$ , the QP density of states can be expanded around its singularity at  $E = \Delta$ :  $E/\sqrt{E^2 - \Delta^2} \approx \sqrt{\Delta/[2(E - \Delta)]}$ . Under this approximation we get

$$x_{\text{QP}} \approx \sqrt{2} \int_0^{\infty} dx \frac{n((1+x)\Delta)}{\sqrt{x}} = n_0 \sqrt{\frac{2\pi k_B T}{\Delta}} e^{-\frac{\Delta}{k_B T}}. \quad (4)$$

When both  $\hbar\omega$  and  $k_B T$  are much smaller than  $\Delta$ , the conductivity is also dominated by the singularity in the QP density of states; as a result, the same approximation as in Eq. (4) leads to the following analytic approximation for the real conductivity:

$$\frac{\sigma_1}{\sigma_N} \approx x_{\text{QP}} \left(\frac{2\Delta}{k_B T}\right)^{3/2} \frac{1}{\sqrt{\pi}} \left(\frac{k_B T}{\hbar\omega}\right) \sinh\left(\frac{\hbar\omega}{2k_B T}\right) \times K_0\left(\frac{\hbar\omega}{2k_B T}\right), \quad (5)$$

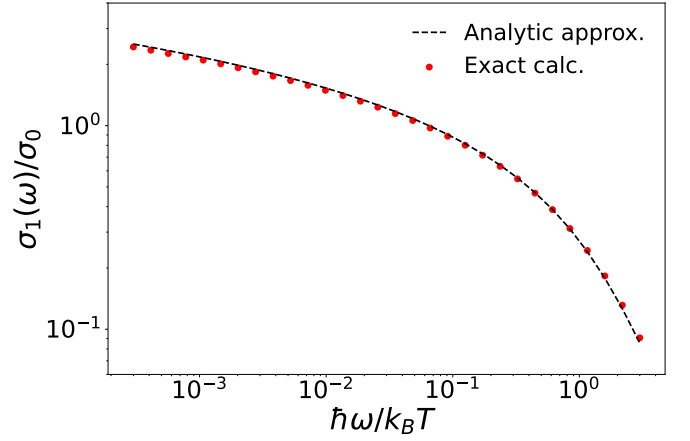


FIG. 1. Numerical calculation of  $\sigma_1(\omega)$  assuming the quasithermal law for the QP distribution observed in experiments,  $n(E) \propto e^{-E/k_B T}$ . The plot is normalized by  $\sigma_0 = \sigma_N x_{\text{QP}} (2\Delta/k_B T)^{3/2}$ . In the low frequency range  $\hbar\omega \lesssim k_B T$ ,  $\sigma_1$  decreases logarithmically with increasing  $\omega$ ; in the high frequency range it decreases as a power law. When  $k_B T \lesssim 0.1\Delta$  we find that the exact numerical result (red points) is well approximated by the analytical expression Eq. (5) (shown as a solid line for comparison).

where  $K_0(y)$  is the modified Bessel function of the second kind.

Figure 1 compares Eq. (5) to exact numerical integration of both Eqs. (2a) and (3), assuming the quasithermal law and  $k_B T/\Delta = 0.1$ . We find that Eq. (5) approximates the exact result quite well provided that  $\hbar\omega, k_B T \lesssim 0.1\Delta$ .

Thus, the behaviour of  $\sigma_1(\omega)$  depends critically on the value of frequency relative to the thermal frequency  $k_B T/\hbar$ . In the low frequency regime of  $\hbar\omega \ll k_B T$ ,  $\sigma_1$  is logarithmic in frequency as

$$\frac{\sigma_1}{\sigma_N} \approx \frac{1}{2\sqrt{\pi}} x_{\text{QP}} \left(\frac{2\Delta}{k_B T}\right)^{3/2} \left[ \ln\left(\frac{4k_B T}{\hbar\omega}\right) - \gamma_E \right], \quad (6)$$

where  $\gamma_E = 0.5772\dots$  is the Euler-Mascheroni constant. In the opposite high-frequency regime of  $\hbar\omega \gg k_B T$ ,  $\sigma_1$  is instead a power law,

$$\frac{\sigma_1}{\sigma_N} \approx \frac{1}{2} x_{\text{QP}} \left(\frac{2\Delta}{\hbar\omega}\right)^{3/2}. \quad (7)$$

The imaginary part of  $\sigma$  has even simpler behaviour, because when  $k_B T \ll \Delta$  we may assume  $[1 - 2n(E + \hbar\omega)] \approx 1$  in Eq. (2b). Thus when  $\hbar\omega, k_B T \ll \Delta$ , we can integrate Eq. (2b) analytically to obtain

$$\frac{\sigma_2}{\sigma_N} \approx \frac{\pi\Delta}{\hbar\omega}. \quad (8)$$

This agrees qualitatively with the phenomenological London theory, which leads to  $\sigma_2^{\text{London}} = \frac{1}{\mu_0 \lambda^2 \omega}$  where  $\mu_0$  is the permeability of vacuum and  $\lambda$  is the penetration

depth. We note that penetration depth  $\lambda$  is often measured using this London expression [23]. Therefore, it makes sense to equate  $\sigma_2^{\text{London}}$  to Eq. (8) in order to obtain

$$\sigma_N = \frac{\hbar}{\mu_0 \lambda^2 \pi \Delta}. \quad (9)$$

This relation, valid for  $\hbar\omega, k_B T \ll \Delta$ , provides a practical method for computing  $\sigma_N$ .

Finally, the impedance generated by QPs can be interpreted as kinetic inductance defined by  $L_k = \text{Re}\{\frac{iZ}{\omega}\}$ . The kinetic inductance due to QPs residing in a wire is then  $L_k = -\text{Im}(\frac{\ell}{A\sigma(\omega)})/\omega \approx \frac{\ell}{A\omega\sigma_2(\omega)}$  since  $\sigma_2(\omega) \gg \sigma_1(\omega)$  at subgap frequencies. Using London's expression for  $\sigma_2$ , we get

$$L_k = \frac{\mu_0 \lambda^2}{A} \ell. \quad (10)$$

We use Eqs. (9) and (10) below for explicit numerical noise estimates as a function of SC parameters.

### III. ENERGY DISTRIBUTION FOR QPS IN QUASIEQUILIBRIUM

A recent experiment presented evidence that SC QPs are at thermal equilibrium with the phonon bath, despite their out-of-equilibrium density. In [17] the following empirical expression for the distribution of QPs in SC circuits was proposed,

$$n(E) = x_{\text{QP}} \sqrt{\frac{\Delta}{2\pi k_B T}} e^{-\frac{E-\Delta}{k_B T}}. \quad (11)$$

Note that this expression follows the quasithermal law mentioned above; in fact Eq. (11) is a Maxwell-Boltzmann distribution with *out-of-equilibrium chemical potential*  $\mu = \Delta$ . The fraction of QPs (normalized by the density of Cooper pairs) is modeled as

$$x_{\text{QP}} = x_{\text{QP}}^{\text{res}} + \sqrt{\frac{2\pi k_B T}{\Delta}} e^{-\frac{\Delta}{k_B T}}, \quad (12)$$

so that the first contribution  $x_{\text{QP}}^{\text{res}}$  is the fraction of QPs that are out of thermal equilibrium, with the second contribution describing QPs at thermal equilibrium. At high temperatures ( $k_B T \geq 100$  mK in [17]), thermal QPs were found to dominate  $x_{\text{QP}}$ , in that  $x_{\text{QP}} \approx \sqrt{2\pi k_B T}/\Delta e^{-\Delta/k_B T}$  leading to  $n(E) \approx f(E)$ . However, at low temperatures, resident QPs with temperature independent density  $x_{\text{QP}}^{\text{res}}$  were found to dominate.

## IV. NOISE IN QUASIEQUILIBRIUM

### A. Charge noise

As is shown in Appendix A, the fluctuation-dissipation theorem remains valid for QP energy distributions that

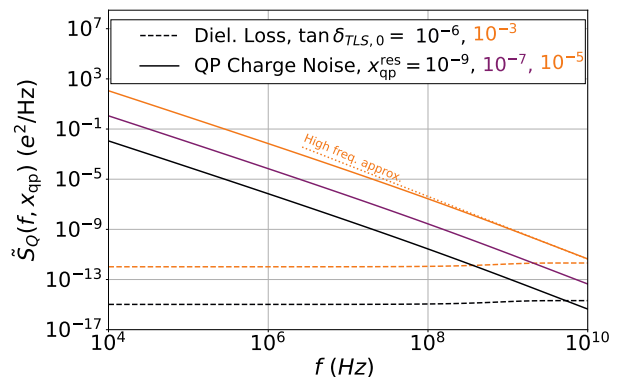


FIG. 2. Charge noise due to quasiequilibrium QPs (solid lines) in Al devices for 3 values of  $x_{\text{QP}}^{\text{res}}$  ranging from  $10^{-9}$  (black) to  $10^{-5}$  (orange). For comparison, charge noise due to dielectric loss assuming typical loss tangents in bulk (black,  $\tan \delta_{\text{TLS},0} = 10^{-6}$ ) and at the surface (orange,  $\tan \delta_{\text{TLS},0} = 10^{-3}$ ) is also shown (dashed lines). The QP high frequency approximation for  $x_{\text{QP}}^{\text{res}} = 10^{-5}$  (dotted line) is shown for comparison. The calculation assumed  $T = 30$  mK and typical SC wire parameters: Wire length  $\ell = 1.5$  mm, cross-sectional area  $A = Wb$  (flat wire) with width  $W = 10$   $\mu\text{m}$  and thickness  $b = 100$  nm, and capacitance per unit length  $C = 168$  pF/m [24]. The normal conductivity  $\sigma_N$  was calculated with Eq. (9) assuming a value of  $\lambda = 50$  nm in Al.

satisfy the “quasithermal law” such as Eq. (11). This implies the charge noise generated by QPs residing in a SC wire is given by

$$\begin{aligned} \tilde{S}_Q(\omega) &= 2\hbar \text{Im}\{\tilde{\chi}_Q(\omega)\} [n_B(\omega) + 1] \\ &= \frac{2\hbar A \sigma_1(\omega)}{\ell \omega} [n_B(\omega) + 1], \end{aligned} \quad (13)$$

where  $n_B(\omega) = 1/(e^{\hbar\omega/k_B T} - 1)$  is the Bose-Einstein distribution. At thermal equilibrium ( $x_{\text{QP}}^{\text{res}} = 0$ ) and  $k_B T \ll \Delta$ , charge noise is exponentially small: E.g. less than  $10^{-30}$   $e^2/\text{Hz}$  above 10 MHz for  $T = 30$  mK for a typical aluminum (Al) SC wire ( $e$  is the electron's charge). In contrast, Fig. 2 shows the charge noise generated by resident QP densities measured in Al devices,  $x_{\text{QP}}^{\text{res}} = 10^{-9} - 10^{-5}$  [14, 17, 25]. We find the QP charge noise is several orders of magnitude higher: E.g. over 20 orders of magnitude larger for  $x_{\text{QP}}^{\text{res}} = 10^{-9}$  compared to thermal QPs at 30 mK in an Al device.

Charge noise scales proportional to  $A/\ell$ , showing that it's more important for small wires. This geometric dependence originates from the charge susceptibility being inversely proportional to the wire's impedance. At low frequencies  $\hbar\omega \ll k_B T$  and low temperatures  $k_B T \ll \Delta$ ,  $x_{\text{QP}}$  is independent of  $T$  and the charge noise scales as  $\tilde{S}_Q(\omega) \propto \ln(4k_B T/\hbar\omega)/(T^{1/2}\omega^2)$ . At high frequencies  $\tilde{S}_Q(\omega) \propto 1/\omega^{5/2}$  is independent of temperature.

In order to quantify the impact of QP charge noise, it is illustrative to compare to dielectric loss originating from two-level system (TLS) defects, one of the main sources of charge noise in SC circuits [26, 27]. The charge noise

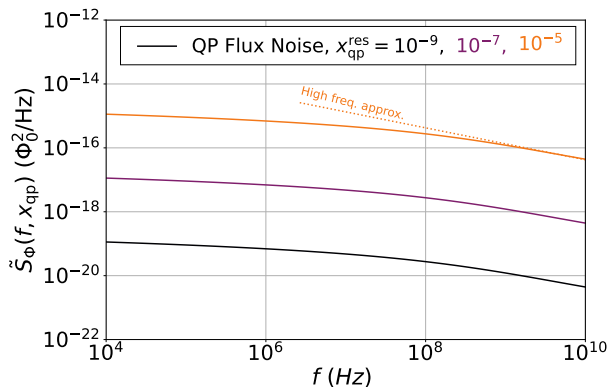


FIG. 3. Flux noise due to quasiequilibrium QPs (solid lines) in Al devices for 3 values of  $x_{\text{QP}}^{\text{res}}$  ranging from  $10^{-9}$  (black) to  $10^{-5}$  (orange). The QP high frequency approximation for  $x_{\text{QP}}^{\text{res}} = 10^{-5}$  (dotted line) is shown for comparison. The calculation assumed  $T = 30$  mK and the same Al SC wire parameters from Fig. 2, plus  $\mathcal{L} = 420$  nH/m.

generated by TLSs can be written as

$$\tilde{S}_Q^{\text{cap}}(\omega) = 2\hbar\mathcal{C}\ell \tan(\delta_{\text{TLS}}) [n_B(\omega) + 1], \quad (14)$$

where  $\mathcal{C} = C/\ell$  is the real part of the wire’s capacitance per unit length, and  $\tan(\delta_{\text{TLS}})$  is the loss tangent due to an ensemble of TLSs. Both  $\mathcal{C}$  and  $\tan(\delta_{\text{TLS}})$  are independent of the wire’s length  $\ell$ . The TLS loss tangent is given by  $\tan(\delta_{\text{TLS}}) = \tan(\delta_{\text{TLS},0}) \tanh(\hbar\omega/2k_B T)$ , with typical amplitudes  $\tan(\delta_{\text{TLS},0}) = 10^{-6}$  and  $10^{-3}$  for TLSs located in the bulk and surface of SC wires, respectively [26, 27]. Figure 2 shows how the TLS bulk and surface contributions compare to QP charge noise in an Al device.

Several experiments focus on measurements of the loss tangent, extracted either from measurements of qubit relaxation rate [26] or from measurements of the quality factor of resonators [27]. In these cases the contribution from QPs is often intertwined with the one from TLSs. For example, in resonator experiments the QP contribution can be extracted from the part of the quality factor that does not increase with increasing power [27]. Comparing Eqs. (13) and (14) we can express the QP mechanism as a loss tangent,

$$\tan(\delta_{\text{QP}}) = \frac{A\sigma_1(\omega)}{\mathcal{C}\ell^2\omega}. \quad (15)$$

While such an interpretation might be useful for comparison, it must be emphasized that the two mechanisms have fundamentally different origin: Dielectric loss corresponds to electrical energy being absorbed into the excitation of TLSs. In contrast, wire-resident QPs are resistive charge carriers, that turn electrical energy into heat due to their scattering into impurities and phonons in the SC wire.

## B. Flux noise

Charge fluctuations lead to current fluctuations, which due to the wire self-inductance  $L$  also gives rise to flux fluctuations with amplitude  $\delta\Phi = L\delta I = -i\omega L\delta Q$ . This implies a flux noise spectral density  $\tilde{S}_\Phi(\omega) = (L\omega)^2 \tilde{S}_Q(\omega)$  is always associated to charge noise. The flux noise generated by nonequilibrium QPs is then

$$\tilde{S}_\Phi(\omega) = 2\hbar\omega\mathcal{L}^2 A\ell\sigma_1(\omega) [n_B(\omega) + 1], \quad (16)$$

where  $\mathcal{L} \equiv L/\ell$  is the wire’s inductance per unit length. Note that flux noise scales proportional to wire length  $\ell$ , the opposite behavior of charge noise (13). At low frequencies ( $\hbar\omega \ll k_B T$ ), flux noise scales logarithmically with frequency and temperature,  $\tilde{S}_\Phi(\omega) \propto \ln(4k_B T/\hbar\omega)/T^{1/2}$ . For not too wide frequency bands this will appear as “nearly white” flux noise. In contrast, for  $\hbar\omega \gg k_B T$ ,  $\tilde{S}_\Phi(\omega) \propto 1/\sqrt{\omega}$ .

Luthi et al. [21] observed a white flux noise background of magnitude  $3.6 \times 10^{-15} \Phi_0^2/\text{Hz}$  of unknown origin in a NbTiN Superconducting Quantum Interference Device (SQUID). Another experiment performed in a different device of the same material measured a similar white flux noise background of magnitude  $2 \times 10^{-16} \Phi_0^2/\text{Hz}$  [28]. Can our proposed QP mechanism explain the origin of this white flux noise background? To try to answer this question, we use our Eq. (16) to estimate the required  $x_{\text{QP}}^{\text{res}}$  that yields the noise level observed in these experiments. From Eq. (10), we estimate a value of kinetic inductance per unit length of the order of 100 nH/m for these devices. Assuming  $\mathcal{L} \approx \mathcal{L}_k$  and other parameters as in [29], we find that  $x_{\text{QP}}^{\text{res}} \sim 10^{-3}$  in Eq. (16) would explain the white flux noise background obtained in both experiments [21, 28].

To our knowledge,  $x_{\text{QP}}^{\text{res}}$  has not yet been measured in NbTiN devices. Instead, an experiment performed in a NbTi resonator measured  $x_{\text{QP}}^{\text{res}} \approx 7 \times 10^{-6}$  [30]. It’s important to note that the QP density depends not only on the material but also on the specific sources driving the electron gas out of equilibrium. Also note that a large geometric inductance, not considered in our calculation, would greatly reduce the estimated  $x_{\text{QP}}^{\text{res}}$ . Therefore, a measurement of  $x_{\text{QP}}^{\text{res}}$  in these devices is needed before reaching a definite conclusion.

Figure 3 shows numerical calculations of flux noise using Eq. (16) for  $x_{\text{QP}}^{\text{res}} = 10^{-9} - 10^{-5}$  for the same Al wire parameters assumed in Fig. 2, plus inductance per unit length  $\mathcal{L} = 420$  nH/m.

For  $x_{\text{QP}}^{\text{res}} = 10^{-9}$ , our predicted amplitude of the “nearly white” flux noise background is of the same order of magnitude as the amplitude measured in flux noise experiments by Quintana et al. [20], in the 10 MHz-1 GHz frequency band with Al devices of similar dimension as in Fig. 3. However, Quintana *et al.* measured a  $1/f$  to  $f$  (Ohmic) flux noise dependence that can not be explained by the present QP mechanism. The low frequency  $1/f$  contribution is likely due to spin impurities [7] and the high frequency Ohmic behaviour remains



unexplained. Nevertheless, the fact that we predict an additional nearly-white QP contribution of similar order of magnitude demonstrates that a flux noise background produced by a nonequilibrium QP density can be a relevant limiting factor in these devices.

## V. CONCLUSIONS

In conclusion, we presented a theoretical model of charge and flux noise due to ohmic loss from resident QPs in SC wires valid for nonequilibrium QP energy distributions. By assuming a quasithermal distribution validated by experimental observations, we estimated the impact of charge noise generated by this mechanism. We found that resident QPs in a SC wire can contribute more to charge noise than dielectric loss generated by TLSs at intermediate frequencies. This contribution will become more relevant as losses from surface TLSs continue to be reduced by better materials and circuit designs [31, 32].

Our model also predicts that a nearly-white flux noise background arises from the out-of-equilibrium QP energy distributions. This provides a possible explanation for the noise background observed in NbTiN devices [21, 28], although additional measurements are needed before a definite conclusion is established. Furthermore, the magnitude of flux noise predicted by our model are found to be comparable to  $1/f$  flux noise levels measured in other devices [20], suggesting the importance of this mechanism as the presence of spin impurities is mitigated [33].

In conclusion, out-of-equilibrium QPs are an important source of charge and flux noise even when the QPs reside away from Josephson junctions. Depending on the magnitude of QP density, the associated noise amplitudes might be larger than well-known mechanisms arising from amorphous two-level systems and spin impurities.

### Appendix A: Fluctuation-Dissipation Theorem for quasiequilibrium distributions

This appendix presents a generalized formulation of the fluctuation-dissipation theorem that shows that it remains valid for quasithermal distributions such as Eq. (11).

Assume a system described by a Hamiltonian  $\mathcal{H}_0$  is perturbed by an external Hamiltonian  $\mathcal{H}_{\text{ext}} = -F(t)\hat{O}$  with  $\hat{O}$  an observable of interest coupled to its conjugate field  $F(t)$ . The *susceptibility operator*  $\hat{\chi}_O$  is defined according to linear-response theory:  $\hat{O}_{F \neq 0}(t) - \hat{O}_{F=0}(t) = \int_{-\infty}^{\infty} dt' \hat{\chi}_O(t-t')F(t')$ . From time-dependent perturbation theory we get  $\hat{\chi}_O(t-t') = \frac{i}{\hbar}\theta(t-t')[\hat{O}(t), \hat{O}(t')]$ , where  $\hat{O}(t) = e^{i\mathcal{H}_0 t/\hbar} O e^{-i\mathcal{H}_0 t/\hbar}$  is the observable in the

interaction picture. In Fourier space

$$\hat{\chi}_O(\omega) = \frac{1}{2\pi\hbar} \int_{-\infty}^{\infty} d\omega' \frac{[\hat{S}_O(-\omega')]^\dagger - \hat{S}_O(\omega')}{\omega - \omega' + i\eta}, \quad (\text{A1})$$

where  $\hat{S}_O(t) = [\hat{O}(t) - \langle \hat{O}(0) \rangle_{\hat{\rho}}][\hat{O}(0) - \langle \hat{O}(0) \rangle_{\hat{\rho}}]$  is the *correlation operator*,  $\hat{S}_O(\omega) = \int_{-\infty}^{\infty} dt e^{i\omega t} \hat{S}_O(t)$  is its Fourier transform and  $\langle \hat{O}(0) \rangle_{\hat{\rho}} = \text{Tr}\{\hat{\rho}\hat{O}(0)\}$  is the average of  $\hat{O}(0)$  at a state described by an arbitrary density matrix  $\hat{\rho}$ .

Equation A1 is an exact operator identity. We now specialize to the case where the system is described by a density matrix that is (1) independent of time (i.e. in a steady state) and (2) diagonal in the basis formed by the energy eigenstates  $\{|E\rangle\}$  of  $\mathcal{H}_0$ :  $\langle E|\hat{\rho}|E'\rangle = \rho(E)\delta_{E,E'}$  with  $\rho(E)$  a real function. Take the average of Eq. (A1) in a such a state and separate its imaginary part to get a *more general version* of the fluctuation-dissipation theorem:

$$2\hbar \text{Im} \left\{ \langle \hat{\chi}_O(\omega) \rangle_{\rho(E)} \right\} = \langle \hat{S}_O(\omega) \rangle_{\rho(E)} - \langle \hat{S}_O(\omega) \rangle_{\rho(E+\hbar\omega)}. \quad (\text{A2})$$

This is based on the identity  $\langle [\hat{S}_O(-\omega')]^\dagger \rangle_{\rho(E)} = \langle \hat{S}_O(\omega) \rangle_{\rho(E+\hbar\omega)}$ , that is valid for a density matrix that satisfies the conditions (1) and (2) above. Note that in Eq. (A2) the quantities  $\langle \hat{\chi}_O(\omega) \rangle_{\rho(E)}$  and  $\langle \hat{S}_O(\omega) \rangle_{\rho(E)}$  are the usual susceptibility and power spectral density of  $\hat{O}$ , respectively; the notation makes their dependence on  $\rho(E)$  explicit.

When  $\hat{\rho}$  satisfies the ‘‘quasithermal law’’  $\hat{\rho} \propto e^{-\mathcal{H}/k_B T}$  we get  $\rho(E + \hbar\omega) = e^{-\hbar\omega/k_B T} \rho(E)$ . This implies  $\langle \hat{S}_O(\omega) \rangle_{\rho(E+\hbar\omega)} = e^{-\hbar\omega/k_B T} \langle \hat{S}_O(\omega) \rangle_{\rho(E)}$ , leading to the usual fluctuation-dissipation theorem:

$$\langle \hat{S}_O(\omega) \rangle_{\rho(E)} = 2\hbar \text{Im} \left\{ \langle \hat{\chi}_O(\omega) \rangle_{\rho(E)} \right\} [n_B(\omega) + 1], \quad (\text{A3})$$

where  $n_B(\omega)$  is the Bose-Einstein distribution. Therefore, the usual fluctuation-dissipation theorem holds for a quasithermal distribution.

## ACKNOWLEDGMENTS

We wish to thank the Engineering Quantum Systems group led by W.D. Oliver at the Massachusetts Institute of Technology for hosting Nava Aquino during part of this work. We acknowledge encouragement and useful discussions with M. Amin, M. Hays, P. Kovtun, W. D. Oliver, K. Serniak, and T. Stavenga. This work was supported by the Natural Sciences and Engineering Research Council of Canada (NSERC) through its Discovery (RGPIN-2020-04328), and its Alliance International Catalyst Quantum Grant (ALLRP-586318-23).

- [1] J. Clarke and F. Wilhelm, Superconducting quantum bits, *Nature* **453**, 1031 (2008).
- [2] J. M. Martinis *et al.*, Decoherence in josephson qubits from dielectric loss, *Phys. Rev. Lett.* **95**, 210503 (2005).
- [3] R. H. Koch, D. P. DiVincenzo, and J. Clarke, Model for  $1/f$  flux noise in squids and qubits, *Phys. Rev. Lett.* **98**, 267003 (2007).
- [4] S. Sendelbach, D. Hover, A. Kittel, M. Mück, J. M. Martinis, and R. McDermott, Magnetism in squids at millikelvin temperatures, *Phys. Rev. Lett.* **100**, 227006 (2008).
- [5] J. Gao *et al.*, A semiempirical model for two-level system noise in superconducting microresonators, *Appl. Phys. Lett.* **92**, 212504 (2008).
- [6] T. Lanting, M. H. Amin, A. J. Berkley, C. Rich, S.-F. Chen, S. LaForest, and R. de Sousa, Evidence for temperature-dependent spin diffusion as a mechanism of intrinsic flux noise in squids, *Phys. Rev. B* **89**, 014503 (2014).
- [7] J. A. Nava Aquino and R. de Sousa, Flux noise in disordered spin systems, *Phys. Rev. B* **106**, 144506 (2022).
- [8] D. C. Mattis and J. Bardeen, Theory of the anomalous skin effect in normal and superconducting metals, *Phys. Rev.* **111**, 412 (1958).
- [9] R. M. Lutchyn, L. I. Glazman, and A. I. Larkin, Kinetics of the superconducting charge qubit in the presence of a quasiparticle, *Phys. Rev. B* **74**, 064515 (2006).
- [10] J. M. Martinis, M. Ansmann, and J. Aumentado, Energy decay in superconducting josephson-junction qubits from nonequilibrium quasiparticle excitations, *Phys. Rev. Lett.* **103**, 097002 (2009).
- [11] G. Catelani, R. J. Schoelkopf, M. H. Devoret, and L. I. Glazman, Relaxation and frequency shifts induced by quasiparticles in superconducting qubits, *Phys. Rev. B* **84**, 064517 (2011).
- [12] G. Catelani, J. Koch, L. Frunzio, R. J. Schoelkopf, M. H. Devoret, and L. I. Glazman, Quasiparticle relaxation of superconducting qubits in the presence of flux, *Phys. Rev. Lett.* **106**, 077002 (2011).
- [13] J. Aumentado, M. W. Keller, J. M. Martinis, and M. H. Devoret, Nonequilibrium quasiparticles and  $2e$  periodicity in single-cooper-pair transistors, *Phys. Rev. Lett.* **92**, 066802 (2004).
- [14] K. Serniak, M. Hays, G. de Lange, S. Diamond, S. Shankar, L. D. Burkhardt, L. Frunzio, M. Houzet, and M. H. Devoret, Hot nonequilibrium quasiparticles in transmon qubits, *Phys. Rev. Lett.* **121**, 157701 (2018).
- [15] S. Diamond, V. Fatemi, M. Hays, H. Nho, P. D. Kurilovich, T. Connolly, V. R. Joshi, K. Serniak, L. Frunzio, L. I. Glazman, and M. H. Devoret, Distinguishing parity-switching mechanisms in a superconducting qubit, *PRX Quantum* **3**, 040304 (2022).
- [16] A. Vepsäläinen, A. Karamlou, J. Orrell, *et al.*, Impact of ionizing radiation on superconducting qubit coherence, *Nature* **584**, 551 (2020).
- [17] T. Connolly, P. D. Kurilovich, S. Diamond, H. Nho, C. G. L. Bøttcher, L. I. Glazman, V. Fatemi, and M. H. Devoret, Coexistence of nonequilibrium density and equilibrium energy distribution of quasiparticles in a superconducting qubit, *Phys. Rev. Lett.* **132**, 217001 (2024).
- [18] T. Yamamoto, Y. Nakamura, Y. A. Pashkin, O. Astafiev, and J. S. Tsai, Parity effect in superconducting aluminum single electron transistors with spatial gap profile controlled by film thickness, *Applied Physics Letters* **88**, 212509 (2006).
- [19] G. Marchegiani, L. Amico, and G. Catelani, Quasiparticles in superconducting qubits with asymmetric junctions, *PRX Quantum* **3**, 040338 (2022).
- [20] C. M. Quintana, Y. Chen, D. Sank, A. G. Petukhov, T. C. White, D. Kafri, B. Chiaro, A. Megrant, R. Barends, B. Campbell, Z. Chen, A. Dunsworth, A. G. Fowler, R. Graff, E. Jeffrey, J. Kelly, E. Lucero, J. Y. Mutus, M. Neeley, C. Neill, P. J. J. O'Malley, P. Roushan, A. Shabani, V. N. Smelyanskiy, A. Vainsencher, J. Wenner, H. Neven, and J. M. Martinis, Observation of classical-quantum crossover of  $1/f$  flux noise and its paramagnetic temperature dependence, *Phys. Rev. Lett.* **118**, 057702 (2017).
- [21] F. Luthi, T. Stavenga, O. W. Enzing, A. Bruno, C. Dickel, N. K. Langford, M. A. Rol, T. S. Jespersen, J. Nygård, P. Krogstrup, and L. DiCarlo, Evolution of nanowire transmon qubits and their coherence in a magnetic field, *Phys. Rev. Lett.* **120**, 100502 (2018).
- [22] J. Gao, *The Physics of Superconducting Microwave Resonators*, Ph.D. thesis, California Institute of Technology (2008).
- [23] T. Hong, K. Choi, K. Ik Sim, T. Ha, B. Cheol Park, H. Yamamori, and J. Hoon Kim, Terahertz electro-dynamics and superconducting energy gap of NbTiN, *Journal of Applied Physics* **114**, 243905 (2013).
- [24] Note, the capacitance per unit length was computed from the zero thickness model [22], assuming a CPW center-strip width to gap width ratio of 1.7 on a silicon substrate.
- [25] P. J. de Visser, J. J. A. Baselmans, P. Diener, S. J. C. Yates, A. Endo, and T. M. Klapwijk, Number fluctuations of sparse quasiparticles in a superconductor, *Phys. Rev. Lett.* **106**, 167004 (2011).
- [26] C. Wang, C. Axline, Y. Y. Gao, T. Brecht, Y. Chu, L. Frunzio, M. H. Devoret, and R. J. Schoelkopf, Surface participation and dielectric loss in superconducting qubits, *Appl. Phys. Lett.* **107**, 162601 (2015).
- [27] N. Gorgichuk, T. Junginger, and R. de Sousa, Modeling Dielectric Loss in Superconducting Resonators : Evidence for Interacting Atomic Two-Level Systems at the Nb /Oxide Interface, *Phys. Rev. Appl.* **19**, 024006 (2023).
- [28] T. Stavenga, *Flux noise in a magnetic field*, Dissertation (tu delft), Delft University of Technology (2023).
- [29] For this calculation, we assume a mixing chamber temperature of  $T=30$  mK.  $T_c = 14.1$  K,  $\lambda=260$  nm for NbTiN [23]. The normal state conductivity  $\sigma_N$  is calculated from Eq. (9). For the device in [21], the wire's length is  $\ell \approx 100$   $\mu\text{m}$ , the width  $W \approx 5$   $\mu\text{m}$ , and the thickness  $b \approx 100$  nm. For the device in [28], the wire's length is  $\ell \approx 30$   $\mu\text{m}$ , the width  $W \approx 2$   $\mu\text{m}$ , and the thickness  $b \approx 100$  nm.
- [30] R. Barends *et al.*, Minimizing quasiparticle generation from stray infrared light in superconducting quantum circuits, *Appl. Phys. Lett.* **99**, 113507 (2011).
- [31] A. P. M. Place, L. V. H. Rodgers, P. Mundada, *et al.*, New material platform for superconducting transmon qubits with coherence times exceeding 0.3 milliseconds,

- [Nat Commun](#) **12**, 1779 (2021).
- [32] J. M. Martinis, Surface loss calculations and design of a superconducting transmon qubit with tapered wiring, [npj Quantum Inf](#) **8**, 26 (2022).
- [33] P. Kumar, S. Sendelbach, M. A. Beck, J. W. Freeland, Z. Wang, H. Wang, C. C. Yu, R. Q. Wu, D. P. Pappas, and R. McDermott, Origin and reduction of  $1/f$  magnetic flux noise in superconducting devices, [Phys. Rev. Appl.](#) **6**, 041001 (2016).